

Article

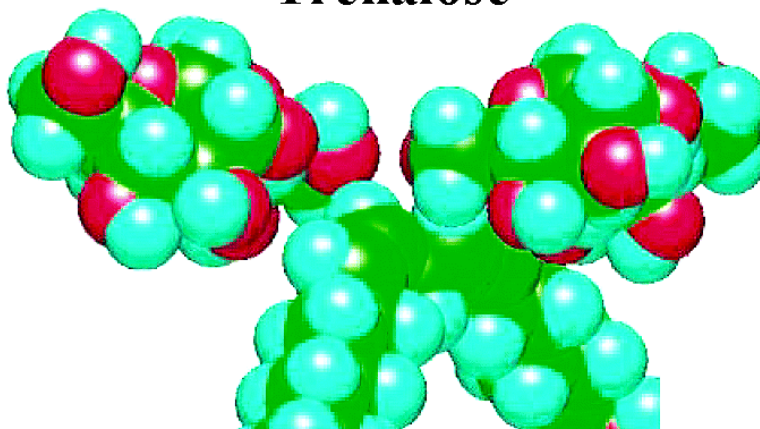
NMR and Quantum Chemical Study on the OH... π and CH...O Interactions between Trehalose and Unsaturated Fatty Acids: Implication for the Mechanism of Antioxidant Function of Trehalose

Kazuyuki Oku, Hikaru Watanabe, Michio Kubota, Shigeharu Fukuda, Masashi Kurimoto, Yoshio Tsujisaka, Masashi Komori, Yoshio Inoue, and Minoru Sakurai

J. Am. Chem. Soc., **2003**, 125 (42), 12739-12748 • DOI: 10.1021/ja034777e • Publication Date (Web): 25 September 2003

Downloaded from <http://pubs.acs.org> on March 30, 2009

Trehalose



Linoleic acid

More About This Article

Additional resources and features associated with this article are available within the HTML version:

- Supporting Information
- Access to high resolution figures
- Links to articles and content related to this article
- Copyright permission to reproduce figures and/or text from this article

[View the Full Text HTML](#)



ACS Publications
High quality. High impact.

NMR and Quantum Chemical Study on the OH $\cdots\pi$ and CH \cdots O Interactions between Trehalose and Unsaturated Fatty Acids: Implication for the Mechanism of Antioxidant Function of Trehalose

Kazuyuki Oku,[†] Hikaru Watanabe,[†] Michio Kubota,[†] Shigeharu Fukuda,[†] Masashi Kurimoto,[†] Yoshio Tsujisaka,[†] Masashi Komori,[‡] Yoshio Inoue,[‡] and Minoru Sakurai^{*‡}

Contribution from the Amase Institute, Hayashibara Biochemical Laboratories, Inc., 7-7 Amaseinami-machi, Okayama 700-0834, Japan, Department of Biomolecular Engineering, Tokyo Institute of Technology, 4259-Nagatsuta-cho, Midori-ku, Yokohama 226-8501, Japan

Received February 20, 2003; E-mail: msakurai@bio.titech.ac.jp

Abstract: Trehalose is a disaccharide that attracts much attention as a stress protectant. In this study, we investigated the mechanism of the antioxidant function of trehalose. The spin–lattice relaxation times (T_1) of ^1H and ^{13}C NMR spectra were measured to investigate the interaction between trehalose and unsaturated fatty acid (UFA). We selected several kinds of UFA that differ in the number of double bonds and in their configurations (cis or trans). Several other disaccharides (sucrose, maltose, neotrehalose, maltitol, and sorbitol) were also analyzed by NMR. The T_1 values for the ^1H and ^{13}C signals assigned to the olefin double bonds in UFA decrease with increasing concentration of trehalose and the changes reaches plateaus at integer ratios of trehalose to UFA. The characteristic T_1 change is observed only for the combination of trehalose and UFA with cis double bond(s). On the other hand, from the ^{13}C – T_1 measurements for trehalose, the T_1 values of the C-3 (C-3') and C-6' (C-6) are found to change remarkably by addition of UFA. ^1H – ^1H NOESY measurements provide direct evidence for complexation of trehalose with linoleic acid. These results indicate that one trehalose molecule stoichiometrically interacts with one cis-olefin double bond of UFA. Computer modeling study indicates that trehalose forms a stable complex with an olefin double bond through OH $\cdots\pi$ and CH \cdots O types of hydrogen bonding. Furthermore, a significant increase in the activation energy is found for hydrogen abstraction reaction from the methylene group located between the double bonds that are both interacting with the trehalose molecules. Therefore, trehalose has a significant depression effect on the oxidation of UFA through the weak interaction with the double bond(s). This is the first study to elucidate the antioxidant function of trehalose.

Trehalose (α -D-glucopyranosyl α -D-glucopyranoside) is a nonreducing disaccharide composed of two glucose molecules joined by an α,α -1,1 linkage. This saccharide occurs widely in nature, microorganisms, plants, and invertebrate animals.¹ The biological role of trehalose in these organisms is known to be not only a reserve carbohydrate but also a bioprotectant against various stresses,^{2–4} such as desiccation, heat, freezing, or osmotic shock. Indeed, it has been demonstrated that trehalose has the ability to stabilize lipid membranes and proteins in vitro.^{5,6} Most recent topics may be the success in preserving frozen or dry mammalian cells using trehalose.^{7,8} In the field

of medicine, evidence has been accumulated that trehalose is superior to other disaccharides in preservation of organ.⁹ On the other hand, a mass-production of trehalose from starch has been developed,¹⁰ and this sugar is extensively used in the fields of food, cosmetic, pharmaceutical, and medicinal industries. Therefore, trehalose is one of the most attractive disaccharides from both scientific and industrial viewpoints.

In addition to the protection function against the water stresses mentioned above, there is growing evidence that trehalose acts as an antioxidant. Lipid peroxidation is a critical factor leading to deterioration in lipid-containing foods during processing, transportation and storage.¹¹ It is of great interest to improve the oxidative stability of lipid-containing foods. Previously, we

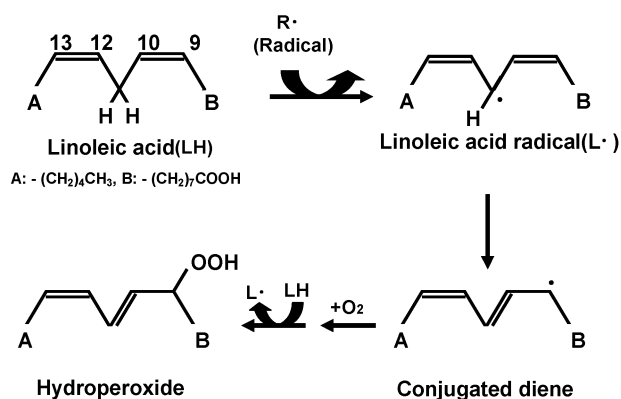
[†] Hayashibara Biochemical Laboratories, Inc.

[‡] Tokyo Institute of Technology.

- (1) Elbein, A. D. *Adv. Carbohydr. Chem. Biochem.* **1974**, *30*, 227.
- (2) Laere, A. V. *FEMS Microbiol. Rev.* **1989**, *63*, 201.
- (3) Singer, M. A.; Lindquist, S. *TIBTECH* **1998**, *16*, 460.
- (4) Argüelles, J. C. *Arch. Microbiol.* **2000**, *174*, 217.
- (5) Crowe, J. H.; Crowe, L. M.; Carpenter, J. F.; Wistrom, C. A. *Biochem. J.* **1987**, *242*, 1.
- (6) Crowe, J. H.; Crowe, L. M.; Carpenter, J. F.; Rudolph, A. S.; Wistrom, C. A.; Spargo, B. J.; Anchordoguy, T. J. *Biochim. Biophys. Acta* **1988**, *947*, 367.

- (7) Eroglu, A.; Russo, M. J.; Bieganski, R.; Fowler, A.; Cheley, S.; Bayley, H.; Toner, M. *Nature Biotech.* **2000**, *18*, 163.
- (8) Guo, N.; Puhlev, I.; Brown, D. R.; Mansbridge, J.; Levine, F. *Nature Biotech.* **2000**, *18*, 168.
- (9) Fukuse, T.; Hirata, T.; Nakamura, T.; Ueda, M.; Kawashima, M.; Hitomi, S.; Wada, H. *Transplantation* **1999**, *68*, 110.
- (10) Chaen, H. J. *Appl. Glycosci.* **1997**, *44*, 115.
- (11) Kaneda, A. *Yukagaku* **1980**, *29*, 295.

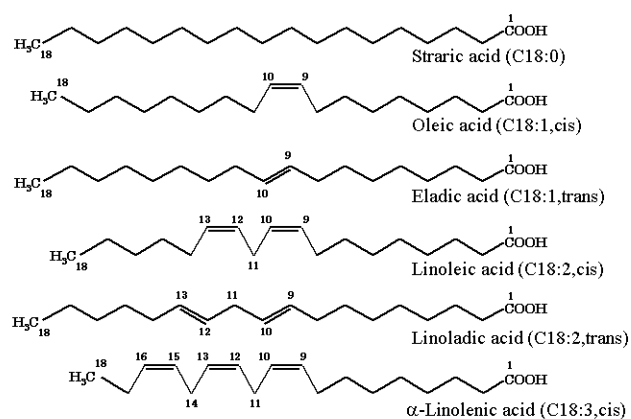
Scheme 1. Peroxidation of Linoleic Acid



reported that trehalose inhibited the heat-induced peroxidation of unsaturated fatty acid (UFA).¹² More recently, we found that this saccharide protects UFA from the oxidation initialized by oxygen radicals.¹³ An *in vivo* study by Benaroudj et al. indicated that trehalose protects yeast cells and cellular proteins from damage by oxygen radicals.¹⁴ The new function of trehalose as an antioxidant is not only useful for industrial application including preservation of food and other biomaterials, but also quite interesting from the viewpoint of fundamental chemistry. However, the molecular mechanism of the antioxidant function of this sugar remains unclear.

It is well-known that the autoxidation of UFA is initialized by the reaction in which activated oxygen or free radicals abstract hydrogen atoms from the allyl group of UFA.¹⁵ Usually, the free radicals are generated by various environmental stimulations such as heat, light, and metals.^{16,17} In the subsequent reaction, called promotion, the resultant conjugated diene reacts with O_2 and another UFA molecule to produce hydroperoxy-fatty acid. Although the hydroperoxy UFA radical is tentatively accumulated in the promotion step, it undergoes degradation or polymerization by the secondary oxidation reaction.¹⁵ The autoxidation and promotion steps are summarized in Scheme 1, where linoleic acid is taken as an example of UFA. Our previous study showed that trehalose greatly depresses the reaction rate of the autoxidation step rather than those of the subsequent reactions.¹³ In addition, other disaccharides, such as sucrose, maltose, and neotrehalose, showed negligible effect on this step. Generally, most of the antioxidants for lipids, such as 2,6-di-*tert*-butyl-4-methylphenol (BHT) or dicarbonic acids, are used as either a radical-scavenger or a metal-sequestrator by chelation.^{18,19} It is known that some sugar alcohols, such as sorbitol and maltitol, have the ability to inhibit the lipid peroxidation by so-called metal chelation effect.^{20,21} However, for trehalose, neither of the radical-scavenger nor metal-sequestrator function has been observed in our previous studies.^{12,13} Thus, there may be another inhibition mechanism

Scheme 2. Structure of C-18 Fatty Acids



specific for trehalose. One possible hypothesis is that trehalose interacts directly with oxidation-sensitive parts of UFA and consequently protects it from the autoxidation.

In this study, to demonstrate this hypothetical mechanism, we first investigate the interaction between trehalose and UFA by measuring the spin-lattice relaxation times of 1H and ^{13}C NMR and 1H - 1H NOESY spectra for a mixture of trehalose and UFA, under the conditions that both components are dissolved together in a water/methanol mixed solvent. We select several kinds of UFA (Scheme 2) that differ in the number of double bonds and in their configurations (cis or trans). An important finding is that trehalose interacts only with the cis double bond in a 1:1 molar ratio. Next, based on quantum chemical calculations, we propose a molecular model that one trehalose molecule binds to one cis-olefin double bond of UFA via $OH\cdots\pi$ and $CH\cdots O$ types of hydrogen bonding. Finally, we will investigate how such hydrogen bonding formation affects the activation energy of hydrogen abstraction reaction that is expected to occur at the allyl position of UFA. Consequently, trehalose significantly increases the activation energy through those interactions with UFA, lowering the rate of oxidation reaction of UFA. The present study is the first one to elucidate the mechanism of antioxidation activity of trehalose.

Materials and Methods

Trehalose (>99.9% purity), maltitol (4-O- α -D-glucopyranosyl-D-sorbitol, 99.3%), neotrehalose (α -D-glucopyranosyl β -D-glucopyranoside, 99.8%) and maltose (4-O- α -D-glucopyranosyl-D-glucose, 99.9%) were produced by Hayashibara Biochemical Laboratories, Inc., Okayama, Japan. Sucrose (α -D-glucopyranosyl β -D-fructofuranoside, >99%) and sorbitol (D-sorbitol, >99%) were purchased from Wako Pure Chemical Industries, Osaka, Japan and Tokyo Chemical Industries Co., Tokyo, Japan, respectively.

Stearic acid (octadecanoic acid, >99%) was purchased from Wako Pure Chemical Industries. Oleic acid (*cis*-9-octadecenoic acid, >99%) was obtained from Tokyo Chemical Industry Co. Linoleic acid (*cis*-9,12-octadecadienoic acid, 99.0%), α -linolenic acid (*cis*-9,12,15-octadecatrienoic acid), eladid acid (*trans*-9-octadecenoic acid, 99.0%), and linoeladid acid (*trans*-9,12-octadecadienoic acid, 99.1%) were purchased from GL Sciences Inc., Tokyo, Japan. These fatty acids were stored in N_2 gas at 4 °C.

The samples for NMR experiments were prepared as follows. First, we separately prepared a solution of UFA and several

(12) Oku, K.; Chaen, H.; Fukuda, S.; Kurimoto, M. *Nippon Shokuhin Kagaku Kougaku Kaishi* (in Japanese) **1999**, *46*, 749.

(13) Oku, K.; Kurose, M.; Kubota, M.; Fukuda, S.; Kurimoto, M.; Tujisaka, Y.; Sakurai, M. *Nippon Shokuhin Kagaku Kougaku Kaishi* (in Japanese) **2003**, *50*, 133.

(14) Benaroudj, N.; Lee, D. H.; Goldberg, L. A. *J. Biol. Chem.* **2001**, *276*, 24 261.

(15) Niki, E. *J. Oleo Sci.* **2001**, *50*, 313.

(16) Terao, J. *J. Oleo Sci.* **2001**, *50*, 393.

(17) Burkitt, M. J.; Gilbert, B. C. *Free Radic. Res. Commun.* **1999**, *10*, 265.

(18) Knight, J. A.; Voorhees, R. P. *Ann. Clin. Lab. Sci.* **1990**, *20*, 347.

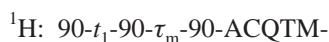
(19) Horikawa, K.; Masuyama, S. *Bull. Chem. Soc. Jpn.* **1971**, *44*, 2697.

(20) Yamaguchi, N.; Ohshima, K.; Murase, M. *Nippon Shokuhin Kagaku Kougaku Kaishi* (in Japanese) **1974**, *21*, 131.

(21) Goldstein, S.; Czapski, G. *Int. J. Radiat. Biol.* **1984**, *46*, 725.

solutions of trehalose with different concentrations. In the case of α -linolenic acid, the former consists of 10 mg (35.6 μ mol) of the fatty acid and 0.9 mL of methanol- d_4 (D, 99.8%, Cambridge Isotope Laboratories, MA), and the latter contains 0, 12.2, 24.4, 36.6 or 48.2 mg (0, 35.6, 71.2, 106.8, or 142.4 μ mol) of trehalose dihydrate and 0.1 mL of deuterium oxide (D, 99.9%, Cambridge Isotope Laboratories, MA). By mixing these solutions, we obtained NMR samples with integer molar ratio between UFA and trehalose. The NMR measurements were done at 25 °C by using an FT-NMR spectrometer (model JMN-AL300, Nihon Denshi Co., Tokyo, Japan), operating at 300.4 MHz (^1H frequency) or 75.45 MHz (^{13}C frequency). The ^1H or ^{13}C chemical shifts (δ) were measured with respect to the ^1H or ^{13}C signal of tetramethylsilane (Wako Pure Chemical Industries) dissolved in the samples, respectively. The ^1H and ^{13}C signal assignments of UFAs were done according to ref 22, and the ^{13}C signal assignments of trehalose according to ref 23.

The spin–lattice relaxation times of ^1H and ^{13}C (hereafter abbreviated as $^1\text{H}-T_1$ and $^{13}\text{C}-T_1$, respectively) were measured using a conventional inversion–recovery pulse sequence, that is, a repeated $90^\circ-\tau-90^\circ$ pulse. The repetition time was taken to be always five times greater than T_1 . For both $^1\text{H}-T_1$ and $^{13}\text{C}-T_1$, the signal recovery was single-exponential decay. The $^1\text{H}-T_1$ measurements were performed for major ^1H peaks assigned to the fatty acids. $^1\text{H}-^1\text{H}$ NOESY spectra were obtained for the mixture of trehalose and linoleic acid (molar ratio of 2:1). NOE measurements were performed using the pulse sequence depicted below



where the mixing time τ_m was taken to be 5 s and the acquisition time ACQTM was taken to be 2.7 s. The NMR data were processed by using a software package, Alice WINNMR 2.1, attached to the NMR apparatus.

Calculation

The MOPAC2000 program²⁴ was used for semiempirical molecular orbital calculations and the Gaussian 98 program²⁵ was used for ab initio and density functional levels of calculation. In computer modeling of intermolecular complexes between trehalose and UFA, the semiempirical AM1 calculation,²⁶ ab initio Hartree–Fock (HF) and density functional theory (DFT) calculations were used. HF and DFT were carried out at the levels of HF/6-31G** and B3LYP/6-31G**, respectively. The search for the transition state in hydrogen abstraction

- (22) Aursand, M.; Rainuzzo, J. R.; Grasdalen, H. *J. Am. Oil Chem. Soc.* **1993**, *70*, 971.
 (23) Asano, N.; Matsui, K.; Takeda, S.; Kono, Y. *Carbohydr. Res.* **1992**, *243*, 71.
 (24) Stewart, J. J. P. MOPAC2000, Fujitsu Ltd., Tokyo, Japan, 1999.
 (25) Frisch, M. J.; Trucks, G. W.; Schlegel, H. B.; Scuseria, G. E.; Robb, M. A.; Cheeseman, J. R.; Zakrzewski, V. G.; Montgomery, J. A., Jr.; Stratmann, R. E.; Burant, J. C.; Dapprich, S.; Millam, J. M.; Daniels, A. D.; Kudin, K. N.; Strain, M. C.; Farkas, O.; Tomasi, J.; Barone, V.; Cossi, M.; Cammi, R.; Mennucci, B.; Pomelli, C.; Adamo, C.; Clifford, S.; Ochterski, J.; Petersson, G. A.; Ayala, P. Y.; Cui, Q.; Morokuma, K.; Malick, D. K.; Rabuck, A. D.; Raghavachari, K.; Foresman, J. B.; Cioslowski, J.; Ortiz, J. V.; Stefanov, B. B.; Liu, G.; Liashenko, A.; Piskorz, P.; Komaromi, I.; Gomperts, R.; Martin, R. L.; Fox, D. J.; Keith, T.; Al-Laham, M. A.; Peng, C. Y.; Nanayakkara, A.; Gonzalez, C.; Challacombe, M.; Gill, P. M. W.; Johnson, B. G.; Chen, W.; Wong, M. W.; Andres, J. L.; Head-Gordon, M.; Replogle, E. S.; Pople, J. A. *Gaussian 98*; Gaussian, Inc.: Pittsburgh, PA, 1998.
 (26) Dewar, M. J. S.; Zoebisch, E. G.; Healy, E. F.; Stewart, J. J. P. *J. Am. Chem. Soc.* **1985**, *107*, 3902.

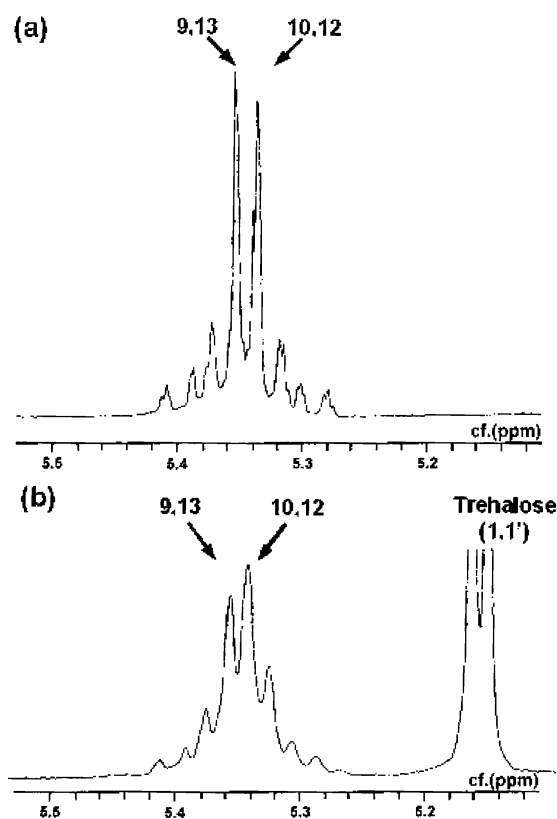


Figure 1. ^1H NMR spectra of linoleic acid olefin protons (H-9, 10, 12, and 13) (a) without trehalose, (b) with trehalose.

reaction was carried out according to a standard protocol (keyword TS), using the UHF/6-31G* and UB3LYP/6-31G* methods.

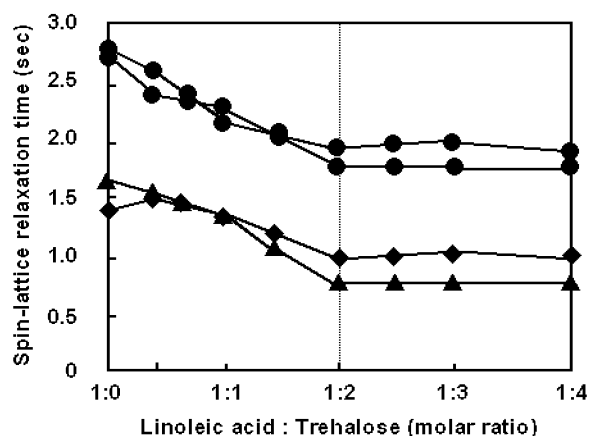
Results

Effect of Sugars on the Relaxation Time of ^1H of Linoleic Acid. Figure 1, parts a and b, shows the ^1H NMR spectra of linoleic acid and a mixture of trehalose and linoleic acid, respectively. In the latter case, the molar ratio of sugar:fatty acid was 2:1. The signals in a range of 5.3–5.4 ppm were assigned to the 9–13 olefin protons of linoleic acid. Their line shapes in the presence of trehalose were broader than those in the absence of the sugar. Similar broadening occurred in the ^1H peaks for the 8, 11, and 14 methylenes, which are adjacent to the double bond in the structure of linoleic acid. However, no apparent changes in line shape were observed for the other ^1H peaks (2 to 7 and 15 to 17 methylenes and 18 methyl). For the above two kinds of samples, we measured the spin–lattice relaxation times of proton signals ($^1\text{H}-T_1$) of linoleic acid and examined the effect of trehalose on the motional property of the fatty acid. As can be seen from Table 1, trehalose caused a remarkable decrease in the $^1\text{H}-T_1$ values of the olefin protons (H-9, 10, 12, and 13) and the adjacent methylenes (H-8, 11, and 14), consistent with the results for the line shape changes as mentioned above. Figure 2 shows the dependence of the $^1\text{H}-T_1$ values of the olefin and the adjacent methylene protons of linoleic acid on the trehalose concentration. Interestingly, the $^1\text{H}-T_1$ vs trehalose concentration curve reaches a plateau at a 2:1 molar ratio of trehalose to linoleic acid. The present NMR measurements were carried out under the so-called extremely narrowing conditions; the decrease of the T_1 value signifies a

Table 1. Effect of Saccharides on the Spin–Lattice Relaxation Time (T_1) of Linoleic Acid Protons

saccharides	spin–lattice relaxation time T_1/s^a					
	H-9,10,12,13	H-11	H-2	H-8,14	H-3,4,5,6,7,15,16,17	H-18
none	2.8	1.7	1.3	1.4	1.3	3.0
trehalose	2.7	0.8	1.2	1.1	1.3	3.0
	1.9					
sucrose	1.8	1.4	1.3	1.4	1.3	2.8
	3.0					
maltose	2.8	1.4	1.3	1.5	1.2	2.8
	2.5					
neotrehalose	2.2	1.4	1.4	1.3	1.3	3.0
	2.7					
maltitol	2.6	1.3	1.4	1.3	1.3	2.7
	2.8					
sorbitol	2.8	1.3	1.3	1.4	1.3	2.8
	2.7					
	2.2					

^a The T_1 measurements were performed at the molar ratio of linoleic acid:sugar = 1:2.

**Figure 2.** Effect of the molar ratio of trehalose to linoleic acid on the relaxation time of the olefin and the adjacent methylene protons. ●: H-9,10,12,13 (olefin protons), ▲: H-11, ◆: H-8,14.

decrease in the mobility of a molecule and/or molecular fragment.²⁷ Thus, the T_1 decrease in the olefin and adjacent methylene protons means the lowering of mobility of the molecular fragments involving the two double bonds and the methylene group interposed between them. Such mobility changes strongly suggest the formation of an intermolecular complex between trehalose and linoleic acid.

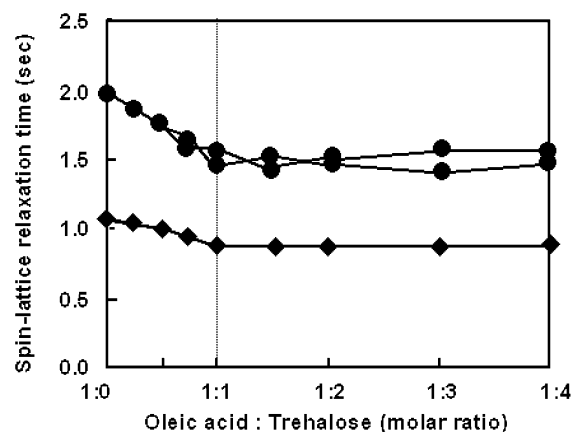
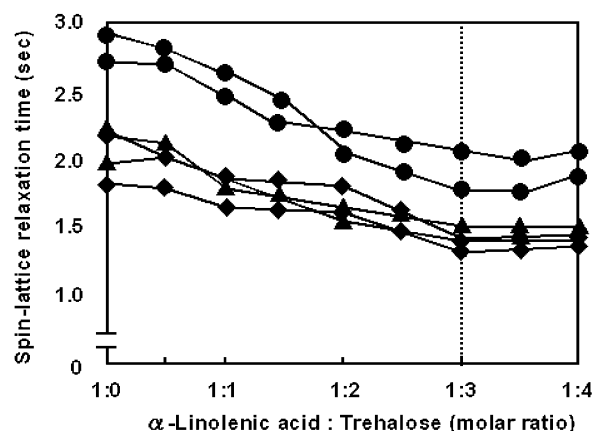
The results for the addition of other saccharides (sucrose, maltose, neotrehalose, maltitol, and sorbitol) are also summarized in Table 1, where all the $^1\text{H}-T_1$ measurements were performed at the molar ratio of sugar:fatty acid = 2:1. These sugars exerted no apparent effect on the T_1 value of all the proton signals of linoleic acid.

To investigate the effect of trehalose on the $^1\text{H}-T_1$ values of fatty acids other than linoleic acid (18:2, cis), we selected stearic acid (18:0), oleic acid (18:1, cis), α -linolenic acid (18:3, cis), eladic acid (18:1, trans) and linoeladic acid (18:2, trans) (see Scheme 2). Table 2 summarizes the $^1\text{H}-T_1$ values of the olefin protons and the protons of the methylene groups interposed between the double bonds. It is again found that trehalose significantly lowers these proton relaxation times but there is no change for sucrose or maltose. In addition, the $^1\text{H}-T_1$ vs trehalose concentration curve reached a plateau at a molar

Table 2. Effect of Saccharides on the Spin–Lattice Relaxation Time (T_1) of α -Linolenic Acid and Oleic Acid

saccharides	spin–lattice relaxation time T_1/s^a				
	α -linolenic acid (C18:3)			oleic acid (C18:1)	
	olefin	adjacent methylene		olefin	adjacent methylene
	H-9,10,12,13,15,16	H-11,14	H-8,17	H-9,10	H-8,11
none	2.7	2.3	2.0	2.0	1.1
	2.9	2.2	1.8	2.0	1.1
trehalose	2.2	1.6	1.8	1.5	0.9
	2.1	1.5	1.6	1.4	0.9
sucrose	2.7	2.2	2.0	2.0	1.0
	2.9	2.2	1.8	2.0	1.1
maltose	2.7	2.2	1.9	2.0	1.0
	2.9	2.2	1.9	2.0	1.1

^a The T_1 measurements were performed at the molar ratio of linolenic acid:sugar = 1:3 and at that of oleic acid:sugar = 1:1.

**Figure 3.** Effect of the molar ratio of trehalose to oleic acid on the relaxation time of the olefin and the adjacent methylene protons. ●: H-9,10 (olefin protons), ◆: H-8,11.**Figure 4.** Effect of the molar ratio of trehalose to α -linolenic acid on the relaxation time of the olefin and the adjacent methylene protons. ●: H-9,10,12,13,15,16 (olefin protons), ▲: H-11,14, ◆: H-8,17.

ratio of trehalose:oleic acid = 1:1 (Figure 3) and at that of trehalose: α -linolenic acid = 3:1 (Figure 4). On the other hand, the $^1\text{H}-T_1$ values of stearic acid, eladic acid and linoeladic acid were barely affected by the addition of trehalose (data not shown).

The above $^1\text{H}-T_1$ results are summarized as follows: (i) trehalose has significant influence on the $^1\text{H}-T_1$ values of the limited types of protons, namely those attached to the cis double bonds of UFA and to those of the methylene groups adjacent to the double bonds, (ii) the saturation points (given by relative

(27) Bloembergen, N.; Purcell, E. M.; Pound, R. V. *Phys. Rev.* **1948**, *73*, 679.

Table 3. Effect of Trehalose on the Chemical Shifts and the Spin–Lattice Relaxation Time (T_1) of Oleic Acid Carbons

	chemical shifts/ppm		spin–lattice relaxation time T_1/s^a	
	without trehalose	with trehalose	without trehalose	with trehalose
C-1	181.4	181.4	n.d.	n.d.
C-9	130.7	130.9	2.0	1.7
C-10	130.6	131.0	1.7	1.4
C-2	34.8	34.8	1.1	1.0
C-16	32.9	32.9	2.5	2.6
C-12,13	30.6	30.6	1.2	1.2
C-14	30.4	30.4	1.7	1.6
C-6	30.3	30.3	1.9	2.0
C-7,15	30.1	30.1	1.2	1.3
C-4,5	30.0	30.0	1.2	1.2
C-8,11	28.0	28.0	1.3	1.3
C-3	25.9	25.9	1.2	1.3
C-17	23.6	23.6	3.1	3.0
C-18	14.4	14.4	4.8	4.6

^a The T_1 measurements were performed at the molar ratio of oleic acid:sugar = 1:1.

molar quantity of trehalose) in the $^1\text{H}-T_1$ vs sugar concentration curves were dependent upon the number of the cis bonds in UFA, (iii) the other sugars studied, including an isomer of trehalose, have no apparent influence on the $^1\text{H}-T_1$ values of any fatty acids studied. Therefore, it can be concluded that $^1\text{H}-T_1$ changes for UFA that were induced by trehalose are caused by interactions between trehalose and the cis double bond of the UFA, and in the resulting intermolecular complex one trehalose molecule binds to one cis double bond.

Effect of Sugars on ^{13}C Spin–Lattice Relaxation Time and Chemical Shifts of UFA. To elucidate the interaction of trehalose with the cis double bond of UFA, we measured the spin–lattice relaxation times of ^{13}C nuclei ($^{13}\text{C}-T_1$) of UFA in the presence of trehalose. The samples used for $^{13}\text{C}-T_1$ measurements contained trehalose in the molar ratios corresponding to the saturation points found in Figures 2–4: namely, trehalose:UFA = 1:1 for oleic acid, 2:1 for linoleic acid, and 3:1 for α -linolenic acid. In the case of oleic acid, the $^{13}\text{C}-T_1$ values of the olefin carbons were 2.0 and 1.7 s for C-9 and C-10, respectively, in the absence of trehalose, while by addition of the sugar the $^{13}\text{C}-T_1$ values were decreased to 1.7 and 1.4 s, respectively (Table 3). Such specific changes for the olefin carbons were also observed for both linoleic acid (Table 4) and α -linolenic acid (Table 5). On the other hand, no significant changes in the $^{13}\text{C}-T_1$ values were observed in stearic acid, eladic acid and linoeladic acid (data not shown), consistent with the results of $^1\text{H}-T_1$ measurements described in the previous section. These results again could suggest that the UFAs possessing cis double(s) bonds alone can interact with trehalose. For all the UFAs studied here, the $^{13}\text{C}-T_1$ values of the methylene carbons adjacent to the double bond, for example, C-8 and C-11 in oleic acid, exhibited no apparent changes by addition of trehalose, although the $^1\text{H}-T_1$ values of the corresponding methylene groups were significantly influenced by the sugar (Tables 1 and 2). In general, the $^1\text{H}-T_1$ value is dependent on both the intra- and intermolecular dipole–dipole relaxation processes.²⁸ The binding of trehalose to a cis olefin double bond probably influences the $^1\text{H}-T_1$ process of the adjacent methylene protons. Thus, combining the $^1\text{H}-T_1$ with $^{13}\text{C}-T_1$ results, we infer that the sites of UFA responsible for

Table 4. Effect of Trehalose on the Chemical Shifts and the Spin–Lattice Relaxation Time (T_1) of Linoleic Acid Carbons

	chemical shifts/ppm		spin–lattice relaxation time T_1/s^a	
	without trehalose	with trehalose	without trehalose	with trehalose
C-1	181.6	181.6	n.d.	n.d.
C-13	130.8	130.9	3.4	2.6
C-9	130.7	131.0	3.4	2.6
C-10	128.9	129.8	3.7	2.7
C-12	128.9	129.8	3.3	2.5
C-2	35.0	35.0	1.3	1.3
C-16	32.5	32.4	4.5	4.1
C-7	30.6	30.6	1.4	1.4
C-6	30.3	30.3	1.6	1.7
C-4,5,15	30.1	30.1	1.5	1.4
C-8,14	28.0	28.0	4.5	4.5
C-11	26.4	26.4	2.2	2.2
C-3	25.9	25.9	2.5	2.4
C-17	23.5	23.5	1.4	1.4
C-18	14.4	14.4	5.1	5.4

^a The T_1 measurements were performed at the molar ratio of linoleic acid:sugar = 1:2.

Table 5. Effect of Trehalose on the Chemical Shifts and the Spin–Lattice Relaxation Time (T_1) of α -Linolenic Acid Carbons

	chemical shifts/ppm		spin–lattice relaxation time T_1/s^a	
	without trehalose	with trehalose	without trehalose	with trehalose
C-1	181.6	181.6	n.d.	n.d.
C-16	132.0	132.5	3.9	3.2
C-9	130.5	130.8	3.3	2.3
C-12,13	128.7	128.9	4.6	4.0
C-10	128.3	128.6	3.1	2.3
C-15	127.8	127.9	3.7	3.1
C-2	34.7	34.7	1.3	1.3
C-7	30.3	30.3	1.7	1.7
C-6	29.9	29.9	1.7	1.7
C-4,5	29.8	29.8	1.7	1.6
C-8	27.8	27.8	2.5	2.5
C-11	26.2	26.2	4.5	4.5
C-14	26.1	26.1	4.6	4.3
C-3	25.7	25.7	1.2	1.3
C-17	21.2	21.2	3.2	3.2
C-18	14.4	14.4	3.5	3.5

^a The T_1 measurements were performed at the molar ratio of α -linolenic acid:sugar = 1:3.

the interaction with trehalose were the cis double bonds themselves rather than the adjacent methylenes.

Tables 3–5 also list the chemical shift data for the UFA molecules with/without trehalose. The chemical shifts of the olefin carbons alone undergo a downfield shift of 0.1–0.9 ppm by addition of trehalose. This strongly supports the above statement.

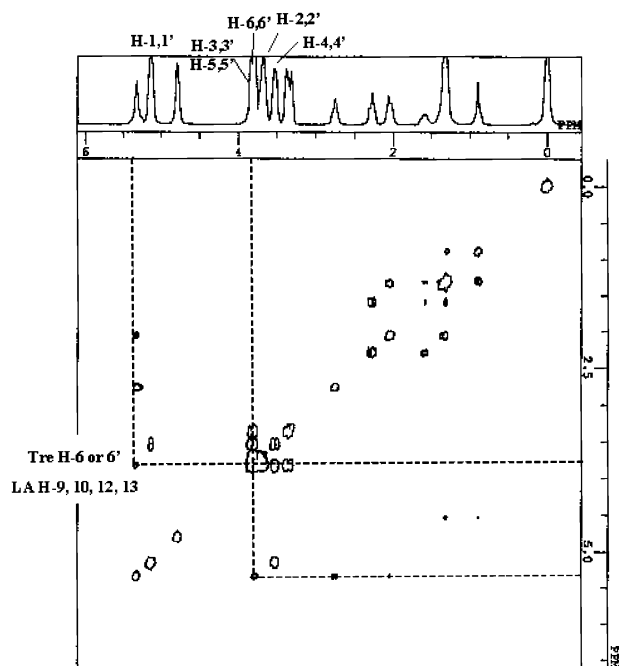
Effect of UFA on ^{13}C Spin–Lattice Relaxation Time and Chemical Shifts of Trehalose. In the present NMR experiments, we could not directly observe the hydroxyl protons of trehalose due to the H–D exchange. Instead, we measured the $^{13}\text{C}-T_1$ s of the sugar to identify the interacting site of trehalose. If the interaction of hydroxyl group of the sugar with UFA has an influence on the mobility of the carbon bound to the hydroxyl group, the interaction should be reflected in the results for the $^{13}\text{C}-T_1$ s of the trehalose carbons. As a result, the $^{13}\text{C}-T_1$ values of trehalose were found to exhibit marked changes only when it was mixed with the UFAs possessing cis double bond(s) (see Table 6). This is quite consistent with the above $^1\text{H}-T_1$ and $^{13}\text{C}-T_1$ results for these UFAs. In particular, the $^{13}\text{C}-T_1$ values of the C-3,3' and C-6,6' atoms were markedly decreased. In the case of linoleic acid, the $^{13}\text{C}-T_1$ values of C-2,2' and C-5,5'

(28) Farrar, T. C.; Becker, E. D. *Pulse and Fourier Transform NMR, Introduction to Theory and Methods*; Academic Press: New York, 1971; Chapter 4.

Table 6. Changes in the Spin–Lattice Relaxation Time (T_1) of Trehalose Carbons Induced by Addition of UFA

chemical shifts /ppm	spin–lattice relaxation time T_1 /ms				
	trehalose	trehalose			
		+ stearic acid ^a	+ oleic acid ^b	+ linoleic acid ^c	+ α -linolenic acid ^d
C-1,1'	354.8	355.2	356.0	347.1	346.5
C-3,3'	369.0	368.4	339.6	332.3	331.5
C-2,2'	322.8	322.5	324.5	307.9	330.6
C-5,5'	352.1	357.8	359.0	333.8	351.0
C-4,4'	330.7	331.0	329.1	360.6	324.3
C-6,6'	219.1	220.2	178.2	180.8	169.5

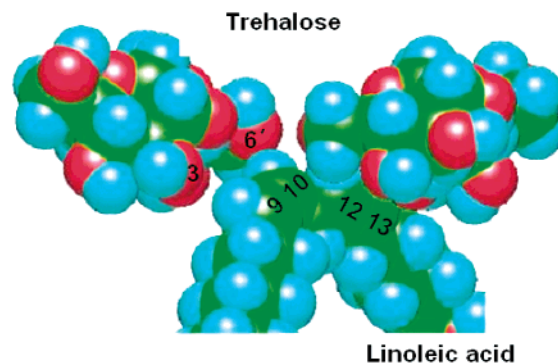
^a The T_1 measurements were performed at the molar ratio of stearic acid:sugar = 1:2. ^b The T_1 measurements were performed at the molar ratio of oleic acid:sugar = 1:1. ^c The T_1 measurements were performed at the molar ratio of linoleic acid:sugar = 1:2. ^d The T_1 measurements were performed at the molar ratio of α -linolenic acid:sugar = 1:3.

**Figure 5.** ^1H – ^1H NOESY spectrum of a mixture of trehalose and linoleic acid (molar ratio = 2:1).

were also slightly decreased and that of C-4,4' was increased. The chemical shifts of C-6,6' and C-3,3' exhibited downfield shifts of 0.2–0.3 and 0.1–0.2 ppm, respectively, by addition of UFA. No apparent chemical shift change was observed for the other carbon atoms. It is thus expected that the OH-3,3' and OH-6,6' groups of trehalose participate in the interaction with the UFAs.

NOE Observation between Trehalose and Linoleic Acid.

To support the results from the ^1H and ^{13}C NMR experiments, we measured the ^1H – ^1H NOESY spectrum of a mixture of trehalose and linoleic acid (molar ratio of 2:1). As can be seen from Figure 5, a clear cross-peak was observed between the 9–13 olefin proton signals (5.3–5.4 ppm) of linoleic acid and the 6(6')-methylene proton signals (3.8 ppm) of trehalose. In this experiment, no apparent cross-peak was observed between the above olefin proton signals and the 3(3')-methine proton signal (3.9 ppm) of trehalose. However, from 1D NOE measurements, a weak NOE was detected for the 3(3')-methine proton when the olefin proton signals was irradiated (data not shown). These results indicate that the interaction at the C-3

**Figure 6.** Plausible model of the interaction between trehalose and linoleic acid. Modeling was carried out by WinMOPAC ver 3.0.

(C-3') site of trehalose is inherently weaker than that at the C-6' site. This will be revealed from quantum chemical calculations as described below.

Computer Modeling for Trehalose-UFA Complexes. The above NMR results indicate that one molecule of trehalose stoichiometrically interacts with one cis-olefinic double bond of UFA, and the OH-6 (OH-6') and OH-3 (OH-3') participate in the interaction. It is of interest to understand the molecular details of this intriguing interaction. First, we examined by computer modeling whether the interaction between these hydroxyl groups of trehalose and the cis-olefin hydrogens of UFA was sterically possible or not. As a result, a plausible model for the trehalose-linoleic acid interaction was obtained as shown in Figure 6, where two molecules of trehalose bind to one linoleic acid, and the OH-3 and OH-6' (or OH-3' and OH-6) of each sugar come into contact with the two CH groups of one cis-olefin double bond. It was also confirmed that the same type of intermolecular complex could be formed between trehalose and oleic acid or α -linolenic acid. Thus, without any steric hindrance more than two trehalose molecules can simultaneously approach the cis double bonds involved in a given UFA.

To evaluate the complex formation energy (or stabilization energy), we carried out quantum chemical calculation for two kinds of model system: in both systems UFA was replaced by 2-butene and trehalose was treated by full atom representation or simply replaced by methanol. In these calculations, the final energies may depend on the conformation of trehalose, which has been extensively studied experimentally^{29–32} and theoretically.^{33–37} Here, we adopted a solution structure determined by a NMR study:³¹ namely, the φ (H1–C1–O1–C1') and ψ (H1'–C1'–O1–C1) angles of the glycosidic bond both were -41° . The initial orientation of the hydroxyl group(s) of trehalose or methanol with respect to the double bond of 2-butene was determined using a graphic interface, and the resulting structures were first optimized by the semiempirical

- (29) Brown, G. M.; Tohrer, D. C.; Berking, B.; Beevers, C. A.; Gould, R. O.; Simpson, R. *Acta Crystallogr.* **1972**, B28, 3145.
 (30) Taga, T.; Senma, M.; Osaki, K. *Acta Crystallogr.* **1972**, B28, 3258.
 (31) Batta, G. J.; Kövér, K. E.; Gervay, J.; Hornyák, M.; Roberts, G. M. *J. Am. Chem. Soc.* **1997**, 119, 1336.
 (32) Duda, C. A.; Stevens, E. S. *J. Am. Chem. Soc.* **1990**, 112, 7406.
 (33) Tvaroška, I.; Václavík, L. *Carbohydr. Res.* **1987**, 160, 137.
 (34) Dowd, M. K.; Reilly, P. J.; French, A. D. *J. Comput. Chem.* **1992**, 13, 102.
 (35) Liu, Q.; Schmidt, R. K.; Teo, B.; Karplus, P. A.; Brady, J. W. *J. Am. Chem. Soc.* **1997**, 119, 7851.
 (36) Engelsen, S. B.; Pérez, S. J. *J. Phys. Chem. B* **2000**, 104, 9301.
 (37) French, A. D.; Johnson, G. P.; Kelterer, A.-M.; Dowd, M. K.; Cramer, C. J. *J. Phys. Chem. A* **2002**, 106, 4988.

Table 7. Energies of the Methanol/2-Butene Complex

systems	energy			$\Delta E_{\text{complex}}$		
	AM1/kcal mol ⁻¹	HF/6-31G**/a.u.	B3LYP/6-31G**/a.u.	AM1/kcal mol ⁻¹	HF/6-31G**/ kcal mol ⁻¹	B3LYP/6-31G**/ kcal mol ⁻¹
methanol	-57.05	-115.05	-115.72			
2-butene	-2.17	-156.12	-157.23			
OH $\cdots\pi$	-60.89	-271.67	-272.96	-1.67	-2.51 (-2.31)	-5.20 (-4.45)
CH \cdots O	-60.18	-271.16	-272.95	-0.96	-0.40 (-0.32)	-0.60 (-0.48)

^a The energies after the BSSE correction are shown in the parentheses.

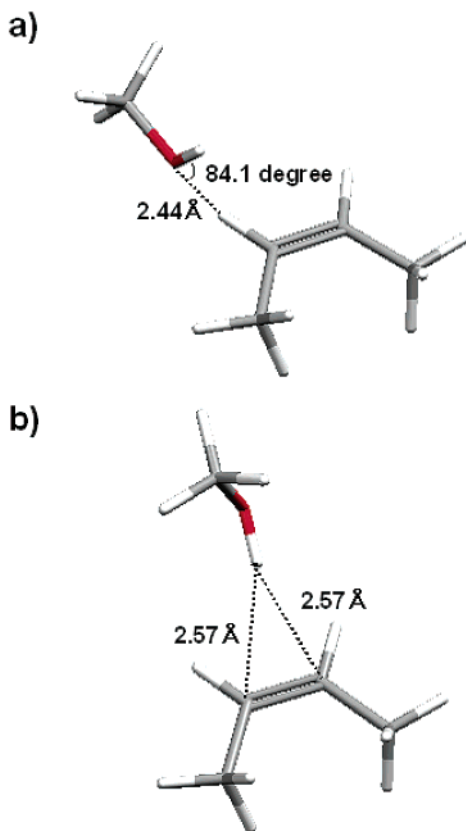


Figure 7. Initial structures assumed for the methanol/2-butene complex. (a) OH $\cdots\pi$ interaction model, (b) CH \cdots O interaction model.

AM1 level of calculation. The geometry optimization at the ab initio HF and DFT levels of theory were started from the resulting AM1 structures. The complex formation energy was obtained as follows

$$\Delta E_{\text{complex}} = E_{\text{complex}} - E_{\text{trehalose or methanol}} - E_{2\text{-butene}}$$

where the first, second and third terms on the right-hand side are the total energies of the complex, trehalose (or methanol) and 2-butene, respectively, and these energies were obtained for the optimized structure of each molecular species. For the ab initio HF and DFT calculations, we performed the correction for basis set superposition errors (BSSE) according to the so-called counterpoise correction procedure.³⁸

In the methanol/2-butene model, we took into account two types of orientation of the alcoholic OH group with respect to the double bond of 2-butene. One is that the oxygen atom is positioned so as to form a hydrogen bond with the CH hydrogen atoms of the double bond on the molecular plane of 2-butene (Figure 7a). The other is that the hydrogen atom of the OH

group attacks the π -orbital of the double bond from the direction perpendicular to the molecular plane (Figure 7b). The former and latter correspond to the C-H \cdots O and O-H $\cdots\pi$ types interaction models, respectively. The calculated results are summarized in Table 7. The AM1 level of calculation indicated that the complex formation energies $\Delta E_{\text{complex}}$ for both models are negative, although the C-H \cdots O interaction model is less stable than the O-H $\cdots\pi$ one. Similarly, the results from the ab initio HF calculations indicated that both types of complex are stable, but the $\Delta E_{\text{complex}}$ for the C-H \cdots O is negligible compared with a thermal energy kT (-0.6 kcal mol⁻¹), where k and T are the Boltzmann constant and temperature ($=300$ K), respectively. The DFT calculation indicated that the O-H $\cdots\pi$ complex alone can be formed with a fairly large stabilization energy ($-\Delta E_{\text{complex}}$) of 5.20 kcal mol⁻¹ (-4.45 kcal mol⁻¹ after the BSSE correction).

Next, we constructed the second model in which trehalose is interacting with 2-butene. According to the above NMR results, the hydroxyl groups of the OH-3' (OH-3) and OH-6 (OH-6') groups were positioned so as to come into contact with the CH groups of the double bond: in more detail, each oxygen atom of these hydroxyl groups was placed so as to have the C-H \cdots O type interaction, similar to Figure 7a. The AM1 geometry optimization calculation starting from such an initial structure gave the final structure which kept the C-H \cdots O type hydrogen bonds at the two CH sites (see Figure 8a). Consistent with the results for the methanol/2-butene model, the AM1 calculation indicated that such an intermolecular complex has a stabilization energy of 1.60 kcal mol⁻¹ (see Table 8). The ab initio HF and DFT optimization calculations starting from this AM1-optimized geometry gave new structures: in both cases, the OH-6' interacts with the π -orbital at the mid position of the double bond and simultaneously the OH-2 forms the C-H \cdots O type of hydrogen bond at a terminal of the double bond (see Figure 8b). The stabilization energies from the ab initio HF and DFT calculations were 5.52 and 7.78 kcal mol⁻¹ before the BSSE correction and 3.41 and 4.49 kcal mol⁻¹ after the correction, respectively.

The conformational changes of trehalose, induced by complexation with 2-butene, are summarized as follows. The HF/6-31G** calculation for the isolated trehalose with φ and $\psi = -41^\circ$ gave the optimized φ and ψ angles of -47.2° and -50.4° , respectively, whereas after the complexation their values were -48.9° and -50.8° . The torsion angles around the O5-C1-O1-C1' and O5'-C1'-O1-C1 were 70.0° and 62.6° in the isolated state, respectively, and 68.8° and 62.9° in the complexed state. These values are similar to other theoretical and experimental data for trehalose, its complexes and derivatives.³⁷ Similar results were obtained from the B3LYP/6-31G** calculation. Therefore, the present calculations indicate that the gauche conformation around the glycosidic bond is kept before and after the complexation. On the other hand, the exocyclic

(38) van Duijneveldt, F. B.; van Duijneveldt-van de Rijdt, J. G. C. M.; van Lenthe, J. H. *Chem. Rev.* **1994**, *94*, 1873.

Table 8. Energies of the Trehalose/2-Butene Complex

systems	energy			$\Delta E_{\text{complex}}$		
	AM1/ kcal mol ⁻¹	HF/6-31G**/a.u.	B3LYP/6-31G**/a.u.	AM1/ kcal mol ⁻¹	HF/6-31G** ^a / kcal mol ⁻¹	B3LYP/6-31G** ^a / kcal mol ⁻¹
trehalose	-541.70	-1290.72	-1297.95			
2-butene	-2.19	-156.12	-157.23			
complex	-545.49	-1446.85	-1455.20	-1.60	-5.52 (-3.41)	-7.78 (-4.49)

^a The energies after the BSSE correction are shown in the parentheses.

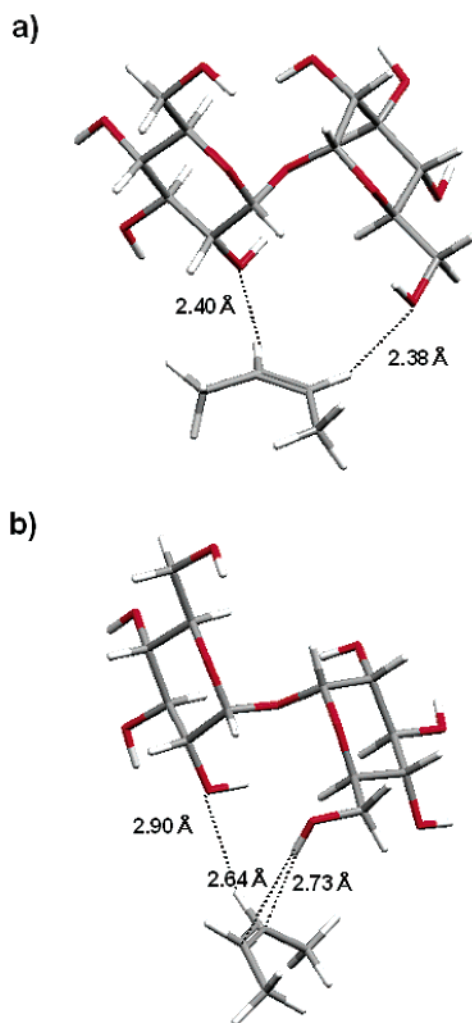
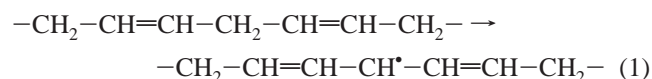


Figure 8. (a) Initial structures assumed for the trehalose/2-butene complex, (b) the optimized structure obtained from the ab initio HF/6-31G** calculation. The HF/6-31G** calculation indicated that for the isolated trehalose the torsion angles around the O5'-C5'-C6'-O6' and C5'-C6'-O6'-H6' bonds were -54.6° and 60.0°, respectively. The values of these torsion angles were changed upon complexation with 2-butene: namely the O5'-C5'-C6'-O6' and C5'-C6'-O6'-H6' torsion angles were 58.7° and -90.2° for (b), respectively.

bond of one glucose ring undergoes a large conformational change to form the O-H... π complex with 2-butene, as described in Figure 8.

Calculation of the Activation Energy of Hydrogen Abstraction Reaction. According to Scheme 1, trehalose depresses the following hydrogen abstraction reaction of UFA



The essential part of the reactant could be modeled using heptadiene. Similarly, as described in the previous section, the

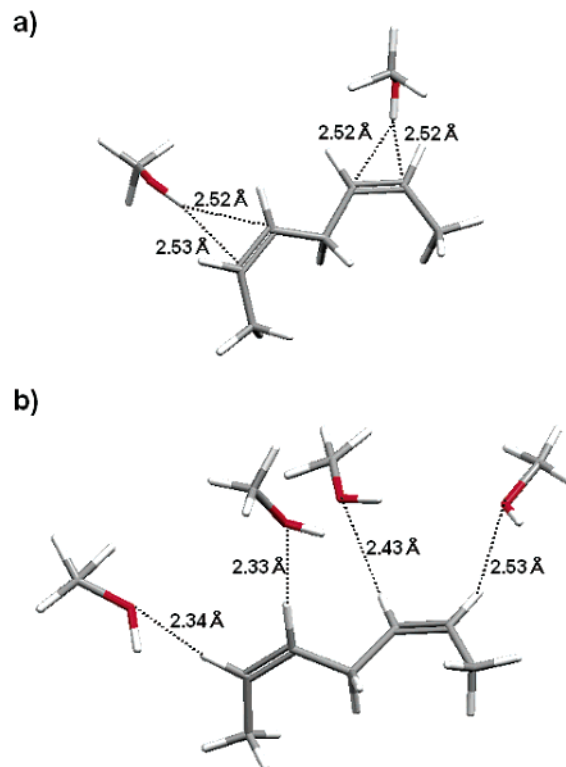


Figure 9. Optimized structure of the methanol/heptadiene complex obtained from the ab initio HF/6-31G** calculation. (a) OH... π interaction model, (b) CH...O interaction model.

hydrogen bonding effect of trehalose can be sufficiently approximated by that of methanol. Thus, two model systems shown in Figure 9, parts a and b, were constructed to evaluate the effect of trehalose on reaction 1. The former has two methanol molecules binding to the two π systems of heptadiene through the O-H... π type interaction, whereas the latter has four methanol molecules binding to the four CH groups through the CH...O type hydrogen bond. In both cases, the stabilization energies $\Delta E_{\text{complex}}$ were evaluated using the B3LYP/6-31G** method. As a result, the $\Delta E_{\text{complex}}$ values per one hydrogen bond were -4.43 and 1.68 kcal mol⁻¹ for the O-H... π and CH...O models, respectively. The value for the O-H... π model is comparable to that (-5.20) given by the 2-butene/methanol model in the previous section (see Table 7). On the other hand, the value for the CH...O model is considerably small compared with that given by the 2-butene/methanol model, indicating that any cooperative effect works in the multi site interaction model as shown in Figure 9a.

For the two interaction models, we obtained the energies of the reactant, transition state and product using the UB3LYP/6-31G** or UHF/6-31G** method. The results are summarized in Table 9. Irrespective of the method used, the activation energy for hydrogen abstraction is significantly increased by the occurrence of interaction with methanol. Interestingly, the rise

Table 9. Calculated Results for Hydrogen Abstraction Reaction of Heptadiene and Heptadiene/Methanol Complexes

method	system	energy/a.u.			activation energy/a.u.	activation energy difference/kcal mol ⁻¹
		reactant	transition state	product		
UB3LYP ^a	heptadiene ^b	-273.9437	-273.8066	-273.3197	0.1371	
	OH... π ^c	-505.4059	-505.2533	-504.7344	0.1526	9.76
	CH...O ^d	-736.8617	-736.7143	-736.1976	0.1474	6.49
UHF ^a	heptadiene ^b	-272.0344	-271.8573	-271.4544	0.1770	
	OH... π ^c	-502.1411	-501.9467	-501.5009	0.1944	10.86
	CH...O ^d	-732.2361	-732.0436	-731.6017	0.1925	9.68

^a 6-31G** basis set was used. ^b Before interaction with methanol. ^c Model shown in Figure 9a ^d Model shown in Figure 9b.

in the activation energy is larger in the O–H... π model than in the CH...O one, despite that the number of the total hydrogen bonds is smaller in the former than in the latter. This indicates that the O–H... π interaction exerts a larger influence on the electronic structure of the diene and the resultant activation energy change amounts to ca. 10 kcal mol⁻¹, about 10% of the activation energy for heptadiene not interacting with methanol. Considering the result of Figure 8b, two molecules of trehalose could bind to heptadiene through a total of four hydrogen bonds including two O–H... π and two CH...O interactions. Then, an increase of at least 10 kcal mol⁻¹ in the activation energy is expected from the results of Table 8. Therefore, it can be safely said that the hydrogen abstraction reaction 1 is significantly depressed by the interaction with trehalose.

Discussion

The above NMR results indicated that one molecule of trehalose stoichiometrically interacts with one cis-olefin double bond of UFA, and the OH-3 (OH-3') and OH-6' (OH-6) hydroxyl groups are responsible for the interaction. It should be noted that such an interaction with UFA was observed only for trehalose, a unique sugar possessing an α,α -1,1 linkage. The quantum chemical calculations revealed that the intermolecular complex between trehalose and 2-butene, a model of cis double bond, can be formed via the C–H...O and O–H... π type interactions with a significant stabilization energy.

Recently, a set of somewhat weaker interactions has been recognized to play an important role in stabilizing protein structures and various types of supermolecular complexes. This set includes C–H...O^{39–44} and O–H... π interactions.^{45–47} In these interactions, the electrostatic contribution to the stability is markedly reduced compared with that in normal hydrogen bond interaction between electron-deficient and electron-rich atoms. Thus, the overall stabilization energy is much smaller, but still significant due to the increase in relative contribution of delocalization energy.⁴⁸ Thus, it is expected that hydroxyl groups of a sugar molecule will form such hydrogen bonds with the olefin double bond(s).

The present quantum chemical calculations were performed using the three methods differing in accuracy: the semiempirical AM1 calculation may be less accurate for the evaluation of hydrogen bonding energy and the DFT calculation would be the most reliable because the electron correlation effect is taken into account. As can be seen from Tables 7 and 8, the stabilization energies, defined as $-\Delta E_{\text{complex}}$, change in order of increasing accuracy: namely, AM1 < ab initio HF < DFT. Interestingly, the O–H... π type of complex becomes more stable in this order, but the C–H...O one becomes unstable (Table 7). If we accept the results only from higher levels of theory (ab initio HF and DFT), it is concluded that the O–H... π type of interaction is more important than the C–H...O one. For the O–H... π type of interaction, the stabilization energies obtained from the ab initio HF and DFT calculations are fairly large compared with the thermal energy kT ($=0.6$ kcal mol⁻¹) at room temperature, although they are smaller than the value (7–8 kcal mol⁻¹) for normal OH...O and NH...O hydrogen bonds.⁴⁸

According to the recent studies based on high levels of calculation that explicitly took into account electron correlation effect,^{45–47} the binding energy of water to the double bond of ethene through the OH... π interaction is ca. 2 kcal mol⁻¹ and that for water dimer is enhanced to ca. -4 kcal mol⁻¹, indicating the presence of cooperative effect. Interestingly, in that water dimer/ethane complex, one water molecule binds to the π bond at the midpoint of the double bond and the oxygen atom of the other does to the CH group through CH...O interaction (see Figure 7b in ref 48). Thus, the way of hydrogen bonding between the water dimer and the ethene molecule is quite similar to that found in the trehalose/2-butene complex (Figure 8b) in this study.

In the present NMR experiments, we used a mixed solvent composed of methanol and water. There is of course a possibility that the solvent molecules bind to the olefin double bond(s) of UFA through the interactions as mentioned above. However, the experiments indicated that trehalose preferentially interacts with the double bond when the molar ratio of trehalose/UFA is increased beyond the integer value corresponding to the number of the double bonds in UFA (Figures 3–5). This phenomenon may be interpreted as follows. As shown in the optimized structure of the trehalose/2-butene complex (Figure 8b), the OH-2 hydroxyl group binds to one of the CH groups of 2-butene through the CH...O type interaction and the OH-6' hydroxyl group does to the double bond through the O–H... π type

(39) Vargas, R.; Garza, J.; Dixon, D. A.; Hay, B. P. *J. Phys. Chem. A* **2000**, *104*, 5115.

(40) Hobza, P.; Šponer, J.; Cubero, E.; Orozco, M.; Luque, F. J. *J. Phys. Chem. B* **2000**, *104*, 6286.

(41) Vargas, R.; Garza, J.; Dixon, D. A.; Hay, B. P. *J. Am. Chem. Soc.* **2000**, *122*, 4750.

(42) Vargas, R.; Garza, J.; Friesner, R. A.; Stern, H.; Hay, B. P.; Dixon, D. A. *J. Phys. Chem. A* **2001**, *105*, 4963.

(43) Raymo, F. M.; Bartberger, M. D.; Houk, K. N.; Stoddart, J. F. *J. Am. Chem. Soc.* **2001**, *123*, 9264.

(44) Bach, R. D.; Thorpe, C.; Dmitrenko, O. *J. Phys. Chem. B* **2002**, *106*, 4325.

(45) Tarakeshwar, P.; Choi, H. S.; Lee, S. J.; Lee, J. Y.; Kim, K. S.; Ha, T.-K.; Jang, J. H.; Lee, J. G.; Lee, H. *J. Chem. Phys.* **1999**, *111*, 5838.

(46) Tarakeshwar, P.; Kim, K. S.; Brutschy, B. *J. Chem. Phys.* **2000**, *112*, 1769.

(47) DuPré, D. B.; Yappert, M. C. *J. Phys. Chem. A* **2002**, *106*, 567.

(48) Brandl, M.; Weiss, M. S.; Jabs, A.; Sühnel, J.; Hilgenfeld, R. *J. Mol. Biol.* **2001**, *307*, 357. The hydrogen bonding strength for the water dimer has been extensively studied so far. The commonly accepted value these days is closer to 5 kcal mol⁻¹. See, for example: Xantheas, S. S.; Dunning, T. H. *J. Chem. Phys.* **1993**, *99*, 8774; Xantheas, S. S. *J. Chem. Phys.* **1994**, *100*, 7523; Xantheas, S. S. *J. Chem. Phys.* **1995**, *102*, 4505.

interaction. Namely, the trehalose interacts with the 2-butene simultaneously at the two sites. As described above, the ab initio HF and DFT results indicated that the former type hydrogen bond is less stable than the latter when each interaction occurs individually. However, a synergistic effect may work when these interactions are simultaneously formed for the same double bond. In fact, if we see the ab initio HF and DFT data before the BSSE correction (Table 8), the stabilization energies ($-\Delta E_{\text{complex}}$) for the complex are larger than the sum of the stabilization energies for the C-H \cdots O and O-H \cdots π interaction models in the methanol/2-butene complex (Table 7). The occurrence of the multiple-site interaction is of greater advantage in entropy than that of individual interactions, which allows the olefin double bond to preferentially interact with trehalose rather than the solvent molecules. In conjunction with this, there is one more reason trehalose is special compared with other sugar molecules. According to a recent quantum chemical study of the intrinsic conformations of trehalose,³⁷ the gauche linkage conformations are 5–7 kcal mol⁻¹ lower in energy than that of the trans shape, consistent with the results from experimental and solution studies.^{31,32} This means that trehalose almost always takes the gauche form at room temperature. Thus, once a multiple interaction occurs for the gauche form of this sugar, it is expected to be kept with a substantial lifetime. The optimized structure shown in Figure 8b satisfies such a condition, because trehalose takes the gauche form as described in the previous section.

The intermolecular complex shown in Figure 8b forms a hydrogen bond at the OH-2 hydroxyl group in addition to the O-H \cdots π bond at the OH-6', whereas the ¹³C NMR results suggested the possibility of interaction at the C-3 (OH-3) position rather than the C-2 (OH-2) one. In fact, we found another intermolecular complex where the OH-3 oxygen atom is binding to the olefin CH without affecting the O-H \cdots π bond at the OH-6' (data not shown). At present, it may be safely said that the OH-6' mainly contributes to formation of the intermolecular complex and the OH-2 or OH-3 group assists the interaction. Detailed comparison between the different interaction models will be discussed elsewhere.

Finally, we discuss the relationship between the present results and the antioxidative activity of trehalose. Our previous studies showed that the heat- or radical-induced peroxidation of UFA was inhibited by addition of trehalose, although the inhibitive activity depended on the concentration of trehalose.^{12,13} Several other disaccharides, such as sucrose, maltose, and neotrehalose, showed negligible effect on the peroxidation, but the activity of maltitol was next to that of trehalose.^{12,13} The chelating action of maltitol on metal ions inhibits the metal-mediated formation of radicals.^{20,21} Probably, the chelating action of maltitol indirectly inhibits the peroxidation of UFA. Thus, among the sugars studied so far, trehalose is the unique antioxidant whose reaction mechanism has not been clarified. We started this study

with the hypothesis that trehalose interacts directly with oxidation-sensitive parts of UFA and consequently protects it from the autoxidation. Now, it is evident from the NMR and quantum chemical data that trehalose can form stable intermolecular complexes with UFA in a unique manner as shown in Figure 8b. In addition, we can also answer a question about to what extent such a direct interaction affects the reaction rate. From the data given in Table 8, it is expected that the activation energy of the hydrogen abstraction reaction 1 is increased by ca. 10 kcal mol⁻¹ when trehalose molecules are binding to the double bonds through the interactions as shown in Figure 8b. According to Arrhenius' equation for reaction rate, this energy change corresponds to lowering of reaction rate by $\sim 10^8$. Therefore, it can be concluded that the hydrogen bonding interaction between trehalose and the olefin double bond, first found in this study, contributes to the antioxidative activity of this sugar.

Concluding Remarks

The present study elucidated the following points: (i) one trehalose molecule interacts specifically with one cis double bond of UFA, (ii) the OH-6' and OH-3 or OH-2 hydroxyl groups are responsible for the interaction, (iii) the complex seems to be stabilized by the multiple-site interaction including the O-H \cdots π and C-H \cdots O types of hydrogen bonds. These new findings are significant advance in understanding the antioxidative activity of trehalose. The interaction of trehalose with polar groups has been extensively investigated so far and trehalose is believed to bind to the polar groups of membrane and protein surface in place of water, called the water replacement hypothesis.^{5,6} However, the present results indicated that the site to which trehalose could bind is not limited to polar groups. As shown in the present study, this property of trehalose is not shared with neotrehalose (α -D-glucopyranosyl β -D-glucopyranoside). Therefore, it is evident that the uniqueness of trehalose comes from the presence of α, α -1,1 linkage by which the sugar is allowed to preferentially take the gauche conformation.⁴⁹

Acknowledgment. We thank Dr. Naoki Asakawa at Tokyo Institute of Technology for his helpful discussion about the NMR data. The authors thank the Computer Center, Institute for Molecular Science, Okazaki, Japan, for the use of the supercomputer system. And we thank the Computer Center, Tokyo Institute of Technology, for the use of the SGI origin 2000 system.

JA034777E

(49) It is known that trehalose does not make any interresidue intramolecular hydrogen bonds in the crystal state (refs 29 and 30), but maltose and sucrose do. A reviewer of this paper suggested that the interresidue bonds in maltose and sucrose might discourage the type of interaction proposed by us for trehalose.